Competing magnetic interactions and interfacial frozen-spins in Ni-NiO core-shell nano-rods

Hao-Chun Hsu, Chih-Chieh Lo, and Yuan-Chieh Tseng

Citation: Journal of Applied Physics **111**, 063919 (2012); doi: 10.1063/1.3699039
View online: http://dx.doi.org/10.1063/1.3699039
View Table of Contents: http://scitation.aip.org/content/aip/journal/jap/111/6?ver=pdfcov
Published by the AIP Publishing

Competing magnetic interactions and interfacial frozen-spins in Ni-NiO core-shell nano-rods

Hao-Chun Hsu, Chih-Chieh Lo, and Yuan-Chieh Tseng[a)]
Department of Materials Science and Engineering, National Chiao Tung University, 1001 Ta Hsueh Road, Hsin-Chu, Taiwan 30010

(Received 13 December 2011; accepted 26 February 2012; published online 29 March 2012)

This paper investigates the subtle interfacial magnetism of highly-aligned, free-standing Ni-NiO core-shell rods on a Si substrate, fabricated by electroless-plating and an anodic aluminum oxide template. Transmission electron microscopy found that the NiO shell was uniformly present along the entire rod. Vertical magnetization shift, arising from opposite field cooling conditions, suggests frozen spins (FS) at the Ni-NiO interface. The FS were related to the pinning effects of the NiO on the Ni. The pinning strength depended on the NiO thickness, displaying a tunable fashion from 6 to 10 nano-meters with thermal annealing. The FS mediated the antiferromagnetic (AFM)-ferromagnetic (FM) interfacial coupling, leading to the temperature-dependent properties of the rods. FS were evident below 100 K, at which the NiO-AFM dominated the properties with a suppressed coercive field and non-saturated magnetization. At 100 K, however, the Ni-FM was superior to the NiO-AFM with a restored FM phase. Meanwhile, the interfacial magnetic frustration occurred due to the disappearance of FS. These two factors resulted in the coercivity enhancement at 100 K. The uniqueness of the structure opens opportunities to tailoring the properties of the rods by manipulating the core-shell inter-dependency, as well as inspiring further researches concerning its applications in spintronics. © *2012 American Institute of Physics*.
[http://dx.doi.org/10.1063/1.3699039]

I. INTRODUCTION

Understanding the fundamental physics underlying the antiferromagnetic (AFM)-ferromagnetic (FM) interactions is essential to the applications in spintronics.[1,2] To further advance spintronics using structures with smaller dimensions, a deeper understanding of the AFM-FM interactions in a variety of nanostructures is necessary. For nanostructured magnetic materials, their macroscopic properties are intimately connected to the vigorous interactions occurring at the AFM-FM interface. Although the correlations between macroscopic properties and interfacial interactions were largely explored in nanostrutcures,[3–8] we noticed that the investigations were less systematic compared to those done in thin films.[9–14] This is mainly due to the nature of poor structural ordering and the difficulty in precisely controlling the AFM-FM interface, for current nanostructures.

Of particular importance, how the two distinct magnets interact within the ordered, 1-dimensional (1-D) configurations[6,7] remains even less conclusive compared to the spherical ones,[3–5,8] due to the effect of anisotropy. Since the longitudinal structure tends to align the moments anisotropically in the axial direction, it could make the manipulation of the interactions more effective than it would be in spherical ones, thus possessing potential applicability in spintronics. Motivated by this cause, efforts were made to fabricate Ni-NiO core-shell rods with high structural ordering to shed some light into the feasibility in this work. The highly-orientated, free-standing nature and tunable AFM/FM in uniformity of the rods can be achieved using a simple fabrication strategy. These advantages successfully isolated the competing AFM-FM interactions and related effects from the rod in a direction-confined manner, making the work distinct from related studies. The uniqueness of the structure also enabled the observation of subtle magnetism such as frozen spins (FS) at the core-shell interface. This allowed us to investigate how the FS mediated the AFM-FM exchange interactions and their evolution with temperature in a systematic fashion. Interestingly, the properties of the rod were shown to be controllable by manipulating the core-shell inter-dependency, thereby providing a playground for the development of similar structures with other tailored properties.

II. EXPERIMENTAL

Ni nano-rods of 70 nm in diameter and 350 nm in height were prepared on a Si substrate using electroless-plating[15] and an anodic aluminum oxide (AAO) template.[16,17] The AAO was then removed, leaving the Ni rods to stand freely on Si.[18] The Ni/Si samples were post-annealed at 350 °C for 15 and 30 min under atmospheric conditions to develop Ni-NiO core-shell structures with different NiO thicknesses. Meanwhile, two sets of Ni reference rods having the same dimensions as the Ni-NiO rods were prepared. The Ni reference samples were heat treated in a similar manner to the Ni-NiO rods but in a nitrogen atmosphere, with AAO to prevent the formation of NiO. We hereafter define the two Ni-NiO samples as NNO-15 and NNO-30, and the two Ni reference samples as N-15 and N-30. The samples were characterized by surface morphology, microstructural, magnetic, and compositional analyses. The surface morphology was

[a)]Author to whom correspondence should be addressed. Electronic mail: yctseng21@mail.nctu.edu.tw.

probed using a scanning electron microscope (SEM). Transmission electron microscopy (TEM) was operated to probe the surfaces of all samples. The phases of Ni and NiO in all samples were examined by selected-area-electron-diffraction (SAED) taken with a fast Fourier transformation (FFT) mode. Energy-dispersive x-ray (EDX) spectroscopy during TEM operation was employed to probe the local atomic percentages of the samples. Magnetic properties were measured along the rod's long axis under various cooling conditions and field strengths using a magnetometer, with the AAO removal. All the magnetic properties excluded Si's contribution.[19]

III. RESULTS AND DISCUSSION

Figure 1(a) presents cross-sectional SEM image of Ni rods standing freely on a Si substrate, which were taken after the removal of the AAO template. As shaped by the AAO, Ni rods were constructed with a dimension of ~350 nm in height and ~70 nm in diameter (aspect ratio = ~5). The dimensions of the four studied samples are identical due to the confinement of the AAO. This allowed us to attribute the differences in probed properties to the annealing conditions. Figure 1(b) shows TEM image of the surface of N-30, where the polycrystalline nature of the rod was transformed from the nano-crystalline microstructure of an as-deposited sample upon annealing. The polycrystalline microstructure promised a ferromagnetic phase as reported by Liu *et al.*[18] The surface of N-15 is very similar to Fig. 1(b) so it is not provided.

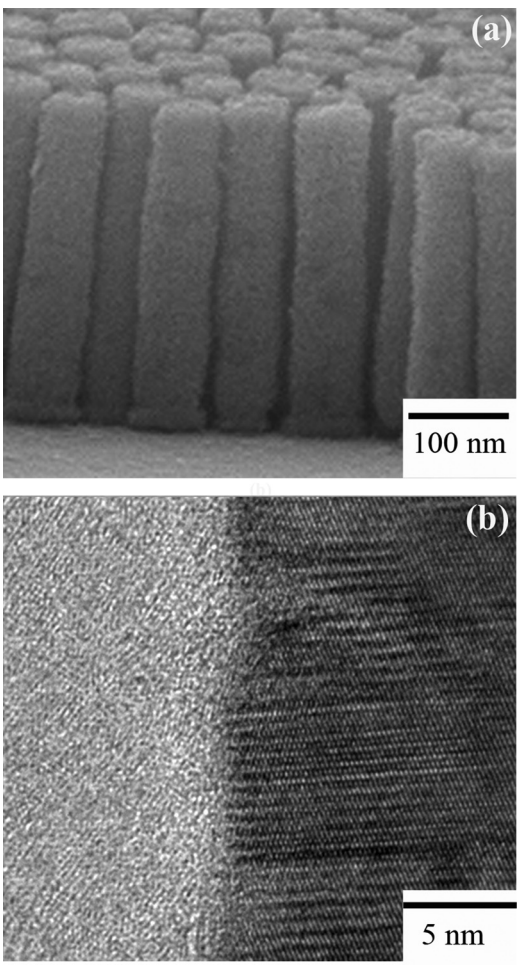

FIG. 1. (a) SEM image of the Ni rods standing freely on a Si substrate. (b) HRTEM image of the surface of the N-30 sample.

Figures 2(a) and 2(b) present TEM images of the surfaces of NNO-15 and NNO-30, respectively, both exhibiting a NiO layer on the Ni surface after annealing. The atomic percentages probed by EDX found the Ni and O concentrations to be 52% and 48%, respectively. The NiO layer was seen elsewhere in the same sample with thickness deviation less than 1 nm, suggesting that the Ni-NiO core-shell structure is present uniformly along the entire rod. This is because the AAO provided excellent rod-isolation that prevented the rods from touching each other during the formation of NiO layer. Nevertheless, a NiO layer is not observed in the N-30 (N-15), as shown in Fig. 1(b), pointing that NiO developed at the expense of Ni via surface oxidation. The thickness of the NiO depended on the duration of annealing, showing approximately 6 and 10 nm for NNO-15 and NNO-30, respectively. Figure 2(c) shows the magnetic hysteresis (M-H) curves of the N-15 (red) and NNO-15 (blue), and Fig. 2(d) presents the same information for the N-30 and NNO-30. Both N-30 and N-15 exhibit FM phases with clearer remnant magnetizations (M_r) and coercive fields (H_c) than the Ni samples reported previously,[20] likely due to the reduced oxidation level because of the use of a nitrogen atmosphere in heat treatment.[21] Although phosphor-based phase such as Ni_3P may appear in the rod due to the use of NaH_2PO_2 in the plating solution,[18] the clear magnetic hysteresis exhibited by N-30 and N-15 indicates that the presence of the Ni_3P influenced the magnetic properties in a very minor way and thus can be neglected.

A larger H_c is exhibited by the N-30 compared to the N-15, revealing a stronger FM ordering facilitated by

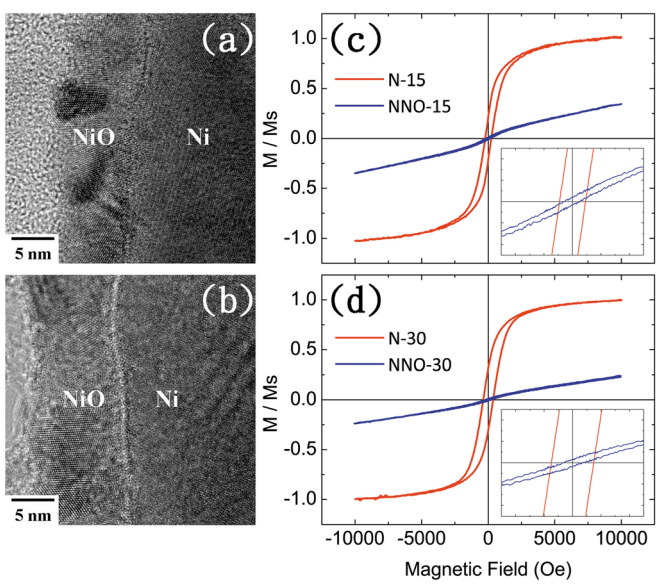

FIG. 2. HRTEM images of (a) NNO-15 and (b) NNO-30. (c) M-H curves of N-15 (red) and NNO-15 (blue) taken at 50 K. (d) M-H curves of N-30 (red) and NNO-30 (blue) taken at 50 K. Insets of (c) and (d) highlight H_c of the rods presented in the main panels.

extended heat treatment. However, suppressed M-H and H_c (insets of Fig. 2(c) and 2(d)) were obtained in the samples in the presence of NiO.[20] The loss of magnetization is due to the oxidation of part of the Ni. Taking NNO-30 as an example, the radius of the FM part reduced from 35 nm to 25 nm compared to N-30, thus in approximation the volume of FM is reduced to half. Although the magnetic suppression has been reported in oxygen-exposed Co clusters,[22] we noticed that it was not observed by Salgueiriño-Maceira *et al*. in Ni-NiO core-shell nanowires deposited on Pt/carbon-nanotubes.[7] Compared to Ref. 7, our core-shell structure is more aligned and structurally uniform and is largely covered by a thicker NiO-shell (our NiO is larger than 6 nm, but the NiO-shell in Ref. 7 is about 2∼3 nm). These structural characteristics greatly facilitated the AFM-screening effect, thus leading to strong magnetic suppression for the rod.

Figures 3(a) and 3(b) present field-cooling (FC) dependent M-H curves for NNO-15 and NNO-30, respectively, obtained after field-cooling (± 3 T) the samples from room temperature down to 50 K. The opposite FC conditions resulted in a vertical shift in magnetization, signaling the existence of frozen spins (FS).[23,24] The FS were likely the result of Ni spins locked to the NiO at the Ni-NiO interface. The FC-dependent M_r values shown in the insets suggest that FS are favored by the +FC, with the magnetization shifted vertically compared to the –FC. It is in highly-oriented core-shell rods we observed the FS, because the randomly-oriented one is inclined to blur the subtle phenomenon.[6,7] A thin NiO layer was able to largely reduce the magnetizations of the Ni samples (Figs. 2(c) and 2(d)), perhaps because the FS fractionally reduced the Ni-FM's degrees of freedom in response to the applied field, therefore further suppressing the magnetization in addition to the AFM-screening effect. The FS were hard to detect along the rod's short axis due to strong demagnetization. The difference in the FC-dependent magnetizations at 1 T is therefore used to quantify the FS, as demonstrated in Fig. 4.

Figures 4(a) and 4(b) illustrate the temperature-dependent FS and H_{ex} curves for the NNO-15 and NNO-30, respectively. The observed H_{ex} arises from the AFM-FM coupling at the Ni-NiO interface. As expected, H_{ex} is proportional to the NiO-AFM thickness as the fact seen in thin film,[25] and it exhibits tunable fashion with annealing condition. However, by looking at the values of H_{ex} of NNO-15 and NNO-30 at 50 K, it is noteworthy that H_{ex} is doubled for an increase of ∼4 nanometers in NiO. This suggests that the exchange anisotropy is particularly strong for the rod, as a result of the high configuration ordering and the uniform coverage of the NiO. Therefore, the structure provides an extra source for exploiting exchange anisotropy compared with the current many nanostructures and ought to inspire further researches concerning its applications

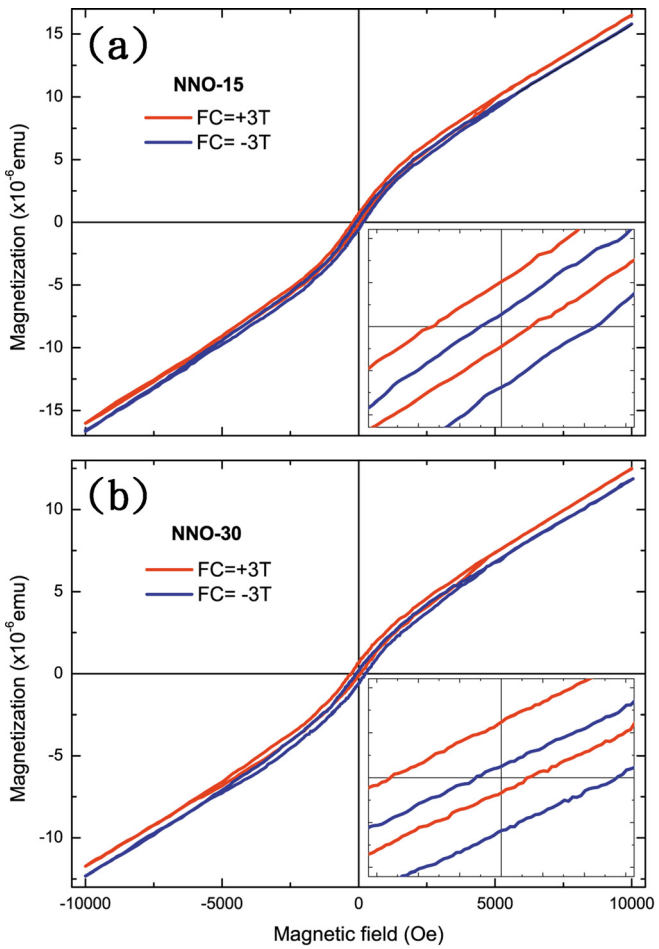

FIG. 3. ± FC M-H curves of (a) NNO-15 and (b) NNO-30. Insets highlight the vertical shifts in the FC-dependent M-H curves for the main panels.

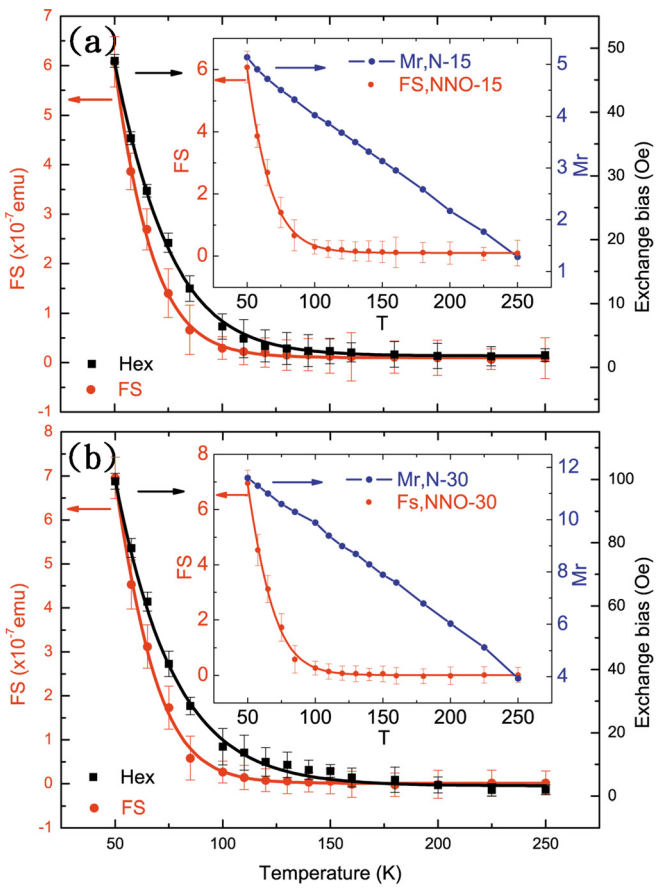

FIG. 4. Temperature-dependent FS (red circles) and H_{ex} (black squares) for (a) NNO-15 and (b) NNO-30. Inset in (a) shows the temperature-dependent FS and M_r of NNO-15 and N-15, respectively. Inset in (b) shows the temperature-dependent FS and M_r of NNO-30 and N-30, respectively.

in spintronics with anisotropic criteria, if the problem of suppressed magnetization can be solved.

In the same plot, the FS-T isolates the temperature-dependency of the locked Ni spins at the interface, which provides critical information for how the interfacial spin structure influences the macroscopic properties of the rod. The FS rapidly drop to nearly zero at approximately 100 K for both NNO-15 and NNO-30, indicating a weakening of the pinning effect of the NiO on warming. The same trend is seen in the H_{ex}-T curve, indicating strong mediation of the FS over the interfacial coupling. Nevertheless, though the FS are closely related to H_{ex}, the FS only increase slightly with the increase of NiO. This is because the FS were collected at a low field (1 T), while the difference in the FS for the two samples was found to increase when a larger collecting field was given. M_r-T curves of the N-15 and N-30 are superimposed onto those of the FS-T of NNO-15 and NNO-30, respectively, as shown in the insets. The M_r-T curve mirrors the temperature-dependency of the Ni FM-ordering without the influence of NiO. The M_rs of the two Ni samples only decrease by approximately 20% from 50 to 100 K. Since the FS disappear at 100 K, the results imply that Ni may dominate the rod's properties above 100 K in the presence of NiO.

Figure 5(a) presents the selected temperature-dependent M-H curves (50, 100, and 300 K) of the NNO-30. The inset highlights H_c for the selected temperatures. The same trend is seen in the NNO-15 (hence, curves are not provided). It can be seen that H_c first increases as the temperature increases from 50 to 100 K, and then decreases after a further temperature increase from 100 to 300 K. At 50 K, the largest H_{ex} and FS (Fig. 4) suggest the dominance of NiO, leading to the suppression of H_c and non-saturated magnetization (Figs. 1(c) and 1(d)). However, at 100 K, a larger H_c and a saturated magnetization indicate the restoration of the FM phase, because Ni begins to dominate the properties of the rods at this temperature. A further decrease in H_c and magnetization following an increase in temperature are simply due to the weakening in the resistance of Ni to warming.

It is noteworthy that at 100 K, the H_c ($\sim$ 420 Oe) of the NNO-30 is larger that of the N-30 ($\sim$280 Oe). This indicates that the increase in H_c from 50 to 100 K cannot be solely attributed to the dominance of Ni. The temperature at which $H_{ex} = 0$ is usually denoted as blocking temperature, T_B, which is 100 K in our case (Fig. 4). The disappearance of H_{ex} at approximately 100 K could be straightforwardly linked to the vanishing of NiO pinning effect on Ni. Above 100 K, the NiO pinning effect and the FS disappeared together, at which the loose NiO spin structures could be reversed by the torque exerted by the Ni spins, and this yielded magnetic frustration at the core-shell interface. It is at 100 K of maximum frustration (i.e., the disappearance of FS and H_{ex}) we observed the largest H_c (Fig. 5(b)). Thus, the enhancement of H_c can be understood in terms of extra coercive strength required to reverse both Ni and NiO. There have been several representative models explaining the enhancement in H_c in exchange-biased systems. These include interfacial magnetic frustration,[10] enhanced higher order anisotropy,[26] reversible (irreversible) changes in AFM spin structure on the reversal of FM layer,[27–29] and

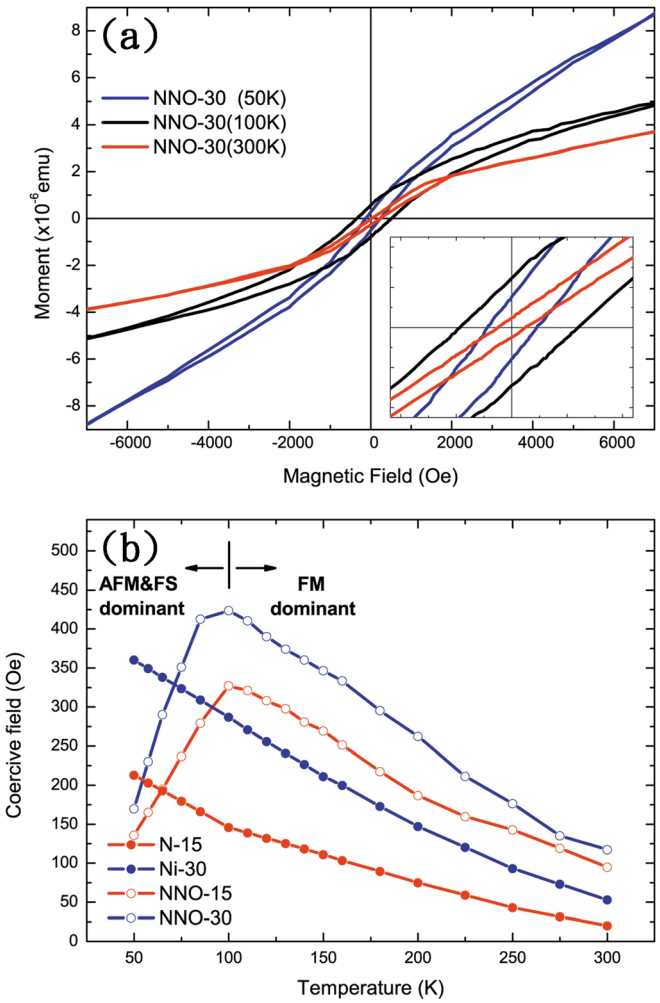

FIG. 5. (a) Selected temperature-dependent magnetic hysteresis curves of NNO-30. (b) Temperature-dependent H_c of N-15 (red filled circles), N-30 (blue filled circles), NNO-15 (red open circles), and NNO-30 (blue open circles). Vertical line on top of the NNO-30 marks the boundary for the AFM- (below 100 K) and FM- (above 100 K) dominant areas.

perpendicular coupling between the AFM and FM layers.[30] Apparently, the coercivity enhancement is a complex subject and the mechanism varies from case to case, depending on the nature of the film/nanostructure. We found that our results are in a similar fashion to Leighton *et al.*[10] who investigated coercivity enhancement driven by interfacial magnetic frustration in a MnF_2/Fe exchange biased system. In their case when the AFM is in a state of maximum frustration and $H_{ex} = 0$, the largest enhancement in H_c is obtained, which supports our conclusion. The temperature-dependent H_c for all of the studied samples are summarized in Fig. 5(b). The sharp increase at 100 K defines the AFM (FM)-dominant boundary and the occurrence of the magnetic frustration, where the reduced (enhanced) H_c for below (at) 100 K reflects the dominance of the AFM (FM). A further increase in temperature resulted in the gradual decay of H_c, similar to the trend seen in the Ni samples, due to thermal instability. We also noticed that the room temperature H_c of the Ni-NiO rods are larger than those of the corresponding Ni ones. This probably arose from the combination of three effects, (i) the reduction of the rod diameter,[31] (ii) decreased

dipolar interactions due to the larger distance between rods,[32] and (iii) the influence of the NiO layer above the blocking temperature.[33]

In summary, we proposed a simple strategy to fabricate AFM-FM core-shell rods, where the rods were highly aligned and their AFM (NiO) shells can be controlled precisely. The work enabled a systematic study of the competing interactions arising from the AFM-FM coupling at the core-shell interface. Also at the interface we observed a close interaction between the FS and the interfacial coupling, responsible for the temperature-dependent properties of the rods. *Microscopically,* the interfacial magnetic frustration occurred simultaneously with the dominance of Ni at 100 K, which resulted in the enhancement in H_c that we observed *macroscopically*.

ACKNOWLEDGMENTS

The authors would like to thank the help of C. M. Liu on TEM data collection. The work was supported by the National Science Council of Taiwan under Grant No. NSC 98-2112-M-009 022-MY3.

[1]W. H. Meiklejohn and C. P. Bean, Phys. Rev. **105**, 904 (1957).
[2]B. Dieny, V. S. Speriosu, S. S. P. Parkin, B. A. Gurney, D. R. Wilhoit, and D. Mauri, Phys. Rev. B **43**, 1297 (1991).
[3]M. Feygenson, Y. Yiu, A. Kou, K. S. Kim, and M. C. Aronson, Phys. Rev. B **81**, 195445 (2010).
[4]K. L. Liu, S. L. Yuan, H. N. Duan, X. F. Zheng, S. Y. Yin, Z. M. Tian, and C. H. Wang, J. Appl. Phys. **107**, 023911 (2010).
[5]J. Nogués, J. Sort, V. Langlais, V. Skumryev, S. Suriñach, J. S. Muñoz, and M. D. Baró, Phys. Rep. **422**, 65 (2005).
[6]T. Maurer, F. Zighem, F. Ott, G. Chaboussant, G. André, Y. Soumare, J-Y. Piquemal, G. Viau, and C. Gatel, Phys. Rev. B **80**, 064427 (2009).
[7]V. Salgueiriño-Maceira, M. A. Correa-Duarte, M. Bañobre-López, M. Grzelczak, M. Farle, L. M. Liz-Marzán, and J. Rivas, Adv. Funct. Mater. **18**, 616 (2008).
[8]M. Gruyters, Phys. Rev. Lett. **95**, 077204 (2005).
[9]J. Nogués, C. Leighton, and Ivan K. Schuller, Phys. Rev. B **61**, 1315 (2000).
[10]C. Leighton, J. Nogués, B. J. Jönsson-Åkerman, and Ivan K. Schuller, Phys. Rev. Lett. **84**, 3466 (2000).
[11]C. Leighton, M. R. Fitzsimmons, A. Hoffmann, J. Dura, C. F. Majkrzak, M. S. Lund, and I. K. Schuller, Phys. Rev. B **65**, 064403 (2002).
[12]J. Nogués, D. Lederman, T. J. Moran, I. K. Schuller, and K. V., Rao, Appl. Phys. Lett. **68**, 3186 (1996).
[13]P. Miltényi, M. Gierlings, M. Bamming, U. May, G. Güntherodt, J. Nogués, M. Gruyters, C. Leighton, and I. K. Schuller, Appl. Phys. Lett. **75**, 2304 (1999).
[14]T. J. Moran, J. Nogués, D. Lederman, and I. K. Schuller, Appl. Phys. Lett. **72**, 617 (1998).
[15]T. K. Tsai and C. G. Chao, Appl. Surf. Sci. **233**, 180 (2004).
[16]M. S. Sander and L. S. Tan, Adv. Funct. Mater. **13**, 393 (2003).
[17]O. Rabin, P. R. Herz, Y. M. Lin, A. I. Akinwande, S. B. Cronin, and M. S. Dresselhaus, Adv. Funct. Mater. **13**, 631 (2003).
[18]C. M. Liu, Y. C. Tseng, C. Chen, M. C. Hsu, T. Y. Chao, and Y. T. Cheng, Nanotechnology **20**, 415703 (2009).
[19]We measured the raw M-H curve (1st) of the sample (rods on Si), and then removed the rods from the Si substrate by mechanical polishing. The remaining sample was examined by SEM to ensure the complete removal of the rods, and then was sent to M-H (2nd) measurement again. We subtracted the 2nd M-H (only Si) from the 1st M-H (Ni on Si) to ensure that the magnetic properties were contributed from the rods alone.
[20]C. C. Lo, C. C. Huang, C. M. Liu, C. Chen, C. Y. Kuo, H. J. Lin, and Y. C. Tseng, J. Magn. Magn. Mater. **323**, 1950 (2011).
[21]The energy-dispersive x-ray spectroscopy found that the Ni rods prepared in a vacuum atmosphere as in Ref. 17, was of ~15% oxidation. However, the Ni rods prepared in a nitrogen condition in this work was only of ~5% oxidation. This is because the vacuum condition of Ref. 17 was low (approximately 10^{-2} torr), so it was difficult to prevent rod's oxidation in heat treatment as compared to the way used in this work.
[22]R. Morel, A. Brenac, and C. Portemont, J. Appl. Phys. **95**, 3757 (2004).
[23]P. H. Huang, H. H. Huang, and C. H. Lai, Appl. Phys. Lett. **90**, 062509 (2007).
[24]R. K. Zheng, G. H. Wen, K. K. Fung, and X. X. Zhang, J. Appl. Phys. **95**, 5244 (2004).
[25]M. S. Lund, W. A. A. Macedo, K. Liu, J. Nogués, I. K. Schuller, and C. Leighton, Phys. Rev. B **66**, 054422 (2002).
[26]Y. J. Tang, B. Roose, T. Mewes, S. O. Demokritov, B. Hillebrands, and Y. J. Wang, Appl. Phys. Lett. **75**, 707 (1999).
[27]M. D. Stiles and R. D. McMichael, Phys. Rev. B **63**, 064405 (2001).
[28]M. D. Stiles and R. D. McMichael, Phys. Rev. B **60**, 12950 (1999).
[29]M. D. Stiles and R. D. McMichael, Phys. Rev. B **59**, 3722 (1999).
[30]T. C. Schulthess and W. H. Butler, Phys. Rev. Lett. **81**, 4516 (1998).
[31]L. P. Carigna, M. Massicotte, C. Caloz, A. Yelon, and D. Menard, IEEE Trans. Magn. **45**, 4070 (2009).
[32]V. Raposo, J. M. Garcia, J. M. González, and M. Vázquez, J. Magn. Magn. Mater. **222**, 227 (2000).
[33]C. Leighton, H. Suhl, M. J. Pechan, R. Compton, J. Nogués, and I. K. Schuller, J. Appl. Phys. **92**, 1483 (2002).